

Measuring nonadiabaticity of molecular quantum dynamics with quantum fidelity and with its efficient semiclassical approximation

Tomáš Zimmermann and Jiří Vaníček^{a)}

Laboratory of Theoretical Physical Chemistry, Institut des Sciences et Ingénierie Chimiques, Ecole Polytechnique Fédérale de Lausanne (EPFL), CH-1015, Lausanne, Switzerland

(Received 1 December 2011; accepted 11 February 2012; published online 2 March 2012)

We propose to measure nonadiabaticity of molecular quantum dynamics rigorously with the quantum fidelity between the Born-Oppenheimer and fully nonadiabatic dynamics. It is shown that this measure of nonadiabaticity applies in situations where other criteria, such as the energy gap criterion or the extent of population transfer, fail. We further propose to estimate this quantum fidelity efficiently with a generalization of the dephasing representation to multiple surfaces. Two variants of the multiple-surface dephasing representation (MSDR) are introduced, in which the nuclei are propagated either with the fewest-switches surface hopping or with the locally mean field dynamics (LMFD). The LMFD can be interpreted as the Ehrenfest dynamics of an ensemble of nuclear trajectories, and has been used previously in the nonadiabatic semiclassical initial value representation. In addition to propagating an ensemble of classical trajectories, the MSDR requires evaluating nonadiabatic couplings and solving the Schrödinger (or more generally, the quantum Liouville-von Neumann) equation for a single discrete degree of freedom. The MSDR can be also used in the diabatic basis to measure the importance of the diabatic couplings. The method is tested on three model problems introduced by Tully and on a two-surface model of dissociation of NaI. © 2012 American Institute of Physics. [<http://dx.doi.org/10.1063/1.3690458>]

I. INTRODUCTION

Nonadiabatic effects give rise to a great variety of phenomena in chemical dynamics.¹⁻³ To account for these effects, many theoretical methods have been developed. The most accurate but also the most computationally demanding are wavepacket approaches which solve the Schrödinger equation for both electrons and nuclei directly. Some wavepacket methods, e.g., the multi-configuration time-dependent Hartree method,^{4,5} have been successfully applied to problems with tens of degrees of freedom. Trajectory based nonadiabatic Bohmian dynamics^{6,7} is another in principle exact method, which can be, moreover, combined with electronic structure computed on the fly.⁸ Less accurate but also less expensive are various semiclassical approaches, which can also describe some quantum effects, especially on the nuclear motion. These include multiple-spawning methods,^{9,10} methods based on the Herman-Kluk propagator,¹¹⁻¹⁴ or the surface hopping and jumping method of Heller *et al.*¹⁵ The most widely used are methods in which the nuclei are treated classically and the quantum effects enter only through interaction with electrons, which are described quantum mechanically. Among these belong methods based directly on the mixed quantum-classical Liouville equation,¹⁶⁻²⁴ the mean field Ehrenfest dynamics, various surface hopping methods,²⁵⁻²⁷ or methods in which the classical limit is obtained by linearizing the path integral representation of the quantum propagator.²⁸

Unfortunately, all of these methods are significantly more computationally demanding than their adiabatic counterparts.

One goal of this paper is to find a general criterion which would determine when a given dynamics is nonadiabatic enough to justify the use of the expensive nonadiabatic methods. Several possible criteria could be envisaged. One widely used criterion is the extent of population transfer or, more precisely, the decay of survival probability P_{QM} on the initially populated potential energy surface (PES) due to nonadiabatic couplings. Although a fast decay of P_{QM} is a clear sign of nonadiabaticity of the dynamics, the opposite implication is not necessarily true: the real extent of nonadiabaticity may be underestimated judging from a relatively modest decay of P_{QM} . Similar effect can be seen in Ref. 29 in the diabatic basis and will be also demonstrated below. Another criterion, often employed to decide when to “switch on” the couplings in nonadiabatic calculations,³⁰ is the energy gap criterion: one simply monitors the energy difference between PESs and when it becomes sufficiently small, the dynamics is considered nonadiabatic. While useful in practical calculations, this criterion does not always reflect the actual extent of nonadiabaticity, which also depends on nonadiabatic couplings and on the nuclear momentum. Other approximate criteria, which are intermediate between the two criteria mentioned, estimate the change of P_{QM} from basic properties of the PESs, from couplings between the PESs, and from the nuclear velocity. Examples include variants³¹ of the Landau-Zener-Stückelberg model.³²⁻³⁶

In Ref. 29, we proposed a more rigorous quantitative criterion of the nonadiabaticity of quantum dynamics in the diabatic basis, which may be easily extended to measure nonadiabaticity in the adiabatic basis. In the latter case, the criterion is based on quantum fidelity F_{QM} ³⁷ between the

^{a)}Electronic mail: jiri.vanicek@epfl.ch.

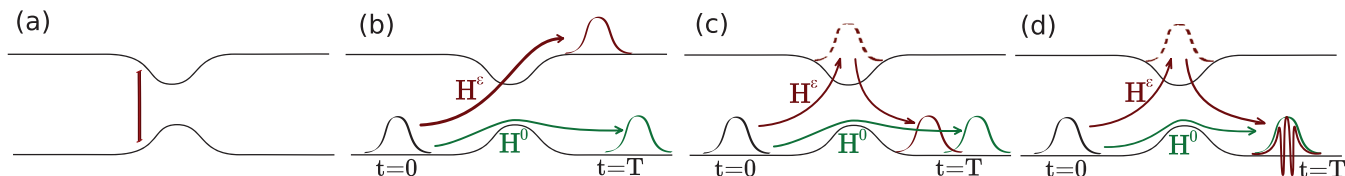


FIG. 1. Possible criteria of nonadiabaticity of quantum dynamics. The static energy-gap criterion does not take into account the dynamics of the wavepacket (a). The population transfer criterion measures the actual decay of probability density on the initial PES (b). It is more sensitive than the static energy-gap criterion. Fidelity criterion can capture the population transfer (b) as well as other nonadiabatic effects such as displacement (c) or interference (d) on a single PES, which would be undetected by the population transfer criterion. \hat{H}^0 is the decoupled Born-Oppenheimer Hamiltonian, whereas \hat{H}^ϵ is the fully coupled nonadiabatic Hamiltonian.

adiabatically and nonadiabatically propagated molecular wavefunctions. More precisely,

$$F_{\text{QM}}(t) = |f_{\text{QM}}(t)|^2 = |\langle \psi^0(t) | \psi^\epsilon(t) \rangle|^2, \quad (1)$$

where $|\psi^0(t)\rangle$ is the quantum state of the molecule evolved using the Born-Oppenheimer adiabatic Hamiltonian \hat{H}^0 with uncoupled PESs and without the diagonal second order couplings, and $|\psi^\epsilon(t)\rangle$ is the quantum state evolved using the fully coupled nonadiabatic Hamiltonian \hat{H}^ϵ . When $F_{\text{QM}} \approx 1$, $|\psi^0(t)\rangle$ is close to $|\psi^\epsilon(t)\rangle$ and an adiabatic simulation is a good approximation to the nonadiabatic simulation. When $F_{\text{QM}} \ll 1$, adiabatic treatment is inadequate and a nonadiabatic method should be used. Unlike the energy gap and population transfer criteria, the fidelity criterion can detect more subtle nonadiabatic effects caused, e.g., by the displacement and/or interference on a single PES surface (see Fig. 1). Panels (c) and (d) of Fig. 1 show two extreme examples in which the nonadiabatic couplings induce a hop to the excited surface followed by a hop back to the ground surface so that at large times, only the ground state is occupied. While the nonadiabatic couplings have no effect on the final survival probability on the ground surface, they have a large effect on the molecular wavefunction since the returning wavepacket may accumulate a time delay (panel c) or a phase (panel d), and hence can have a zero overlap with the wavepacket propagated adiabatically. Although neither case can be detected by the survival probability criterion, both scenarios can be detected easily by fidelity (1).

The remaining (but difficult) question is how to compute F_{QM} . The most straightforward way would be to propagate the wavefunctions with some wavepacket method and to use Eq. (1) directly. This approach, however, suffers from the previously mentioned disadvantages of wavepacket methods. Instead, below we derive an accurate, yet efficient semiclassical method capable of computing not only fidelity F_{QM} but also fidelity amplitude f_{QM} . The method, which we refer to as the *multiple-surface dephasing representation* (MSDR), is a generalization of the dephasing representation (DR),^{38–40} derived for the adiabatic dynamics using the Van Vleck propagator. In the single surface setting, the DR is closely related to the semiclassical perturbation approximation of Miller and co-workers^{41,42} and to the phase averaging of Mukamel.⁴³ Its main applications include calculations of electronic spectra^{43–49} and evaluations of stability of quantum dynamics.^{39,40,50–52} The main advantage of the MSDR compared to wavepacket methods is that the computational cost of MSDR does not scale exponentially with the number of de-

grees of freedom. Such property has been proven rigorously for the original DR.⁵³ The MSDR can, therefore, be applied to problems with dimensionality far beyond the scope of current methods of quantum dynamics. The advantage of MSDR in comparison with most other semiclassical approaches is that the MSDR does not require the Hessian of the potential energy, which is often the most expensive part of semiclassical calculations (see, e.g., Ref. 54). Finally, in contrast to methods treating the motion of nuclei completely classically, the MSDR includes some nuclear quantum effects approximately via the interference between the classical trajectories representing a wavepacket.

The MSDR is not the first extension of the DR to nonadiabatic dynamics. In Ref. 29, we have introduced another extension of the DR, which is here referred to as the *integral multiple-surface dephasing representation* (IMSDR) and which performs satisfactorily in the case of nearly diabatic dynamics in the diabatic basis. Unfortunately, the accuracy of the IMSDR deteriorates when the dynamics is far from the diabatic limit. Another important limitation of the IMSDR is that it cannot be used in the adiabatic basis. Below we shall demonstrate that the MSDR is both more accurate and more general than the IMSDR. A small price to pay for this improvement is that in contrast to the IMSDR, in which fidelity is computed as an interference integral at the end of dynamics, in the MSDR the Liouville-Von Neumann equation for one discrete (collective electronic) degree of freedom has to be solved during the dynamics. For pure states, this equation is simple and is equivalent to the Schrödinger equation for one discrete degree of freedom which is already solved during the Ehrenfest or fewest switches surface hopping (FSSH) dynamics. Both MSDR and IMSDR reduce to the original DR for systems with a single PES.

The outline of the paper is as follows: in Sec. II, the MSDR is derived. In Sec. III, the method is used to evaluate nonadiabaticity of quantum dynamics in several model systems. For the sake of comparison with the previously introduced IMSDR method, the MSDR is also used to evaluate nonadiabaticity in the diabatic basis set. Computational details are summarized in the same section. Section IV concludes the paper.

II. THEORY

A. MSDR

A starting point for the derivation of the MSDR is the expression for quantum fidelity amplitude formulated in terms

of the density matrix⁴⁰

$$f_{\text{QM}}(t) = \text{Tr}(e^{-i\hat{\mathbf{H}}^\epsilon t/\hbar} \cdot \hat{\rho}^{\text{init}} \cdot e^{+i\hat{\mathbf{H}}^0 t/\hbar}), \quad (2)$$

where $\hat{\rho}^{\text{init}}$ is the density operator of the initial state, $\hat{\mathbf{H}}^0$ and $\hat{\mathbf{H}}^\epsilon$ are two different molecular Hamiltonians expressed either in the diabatic or adiabatic basis. (**Bold** face denotes $n \times n$ matrices acting on the Hilbert space spanned by n electronic states, hat $\hat{\cdot}$ denotes nuclear operators.) Note that Eq. (2) applies to both pure and mixed states.⁴⁰ Formally, $\hat{\mathbf{H}}^\epsilon$ can be written as $\hat{\mathbf{H}}^\epsilon = \hat{\mathbf{H}}^0 + \epsilon \hat{\mathbf{V}}$, where ϵ controls the extent of the perturbation. Expressing f_{QM} in the interaction picture gives

$$f_{\text{QM}}(t) = \text{Tr}(\hat{\rho}^{\text{init}} \cdot \hat{\mathbf{E}}(t)), \quad (3)$$

where

$$\hat{\mathbf{E}}(t) := e^{+i\hat{\mathbf{H}}^0 t/\hbar} \cdot e^{-i\hat{\mathbf{H}}^\epsilon t/\hbar} = \mathcal{T} e^{-i\epsilon \int_0^t \hat{\mathbf{V}}^l(t') dt'/\hbar} \quad (4)$$

is the echo operator^{50,55} and

$$\hat{\mathbf{V}}^l(t) = e^{i\hat{\mathbf{H}}^0 t/\hbar} \cdot \hat{\mathbf{V}} \cdot e^{-i\hat{\mathbf{H}}^0 t/\hbar} \quad (5)$$

is the perturbation in the interaction picture. A partial Wigner transform⁵⁶ of Eq. (3) over nuclear degrees of freedom yields an alternative exact expression for the fidelity amplitude,

$$f_{\text{QM}}(t) = h^{-D} \text{Tr}_e \int dX \rho_{\text{W}}^{\text{init}}(X) \cdot \mathbf{E}_w(X, t), \quad (6)$$

where $\mathbf{A}_w(X)$ is the partial Wigner transform of operator $\hat{\mathbf{A}}$,

$$\mathbf{A}_w(X) = \int d\xi \left\langle Q - \frac{\xi}{2} \left| \hat{\mathbf{A}} \right| Q + \frac{\xi}{2} \right\rangle \exp\left(i \frac{\xi \cdot P}{\hbar}\right), \quad (7)$$

X denotes the point (Q, P) in the $2D$ -dimensional phase space, and Tr_e is the trace over electronic degrees of freedom. Direct evaluation of the Wigner transform of the echo operator is unfortunately difficult without approximations. As the first approximation, one may truncate the Taylor expansion of the exponential operator in the Wigner transform of a product of two operators

$$\begin{aligned} (\hat{\mathbf{A}} \cdot \hat{\mathbf{B}})_w &= \exp\left(\frac{i\hbar}{2} \{.,.\}\right) (\mathbf{A}_w, \mathbf{B}_w) \\ &= \mathbf{A}_w \exp\left[\frac{i\hbar}{2} \left(\overleftarrow{\frac{\partial}{\partial Q}} \overrightarrow{\frac{\partial}{\partial P}} - \overleftarrow{\frac{\partial}{\partial P}} \overrightarrow{\frac{\partial}{\partial Q}} \right)\right] \mathbf{B}_w \end{aligned} \quad (8)$$

after the zeroth-order term. In Eq. (8), $\{\mathbf{A}, \mathbf{B}\} = \frac{\partial \mathbf{A}}{\partial P} \cdot \frac{\partial \mathbf{B}}{\partial Q} - \frac{\partial \mathbf{A}}{\partial Q} \cdot \frac{\partial \mathbf{B}}{\partial P}$ is the Poisson bracket over the nuclear degrees of freedom and arrows indicate on which argument the derivatives act. An iterative application of expansion (8) to the echo operator (4) expressed as a time-ordered product of the short time propagators gives

$$(\mathcal{T} e^{-i\epsilon \int_0^t \hat{\mathbf{V}}^l(t') dt'/\hbar})_w \simeq \mathcal{T} e^{-i\epsilon \int_0^t \mathbf{V}_w^l(X, t') dt'/\hbar}. \quad (9)$$

To evaluate this expression, the time evolution of $\mathbf{V}_w^l(X, t)$ is required. The second approximation involves replacing the exact equation of motion by a mixed quantum-classical (MQC) propagation scheme described below, leading to the

final expression for MSDR of fidelity amplitude,

$$\begin{aligned} f_{\text{MSDR}}(t) &= h^{-D} \text{Tr}_e \int dX \rho_{\text{W}}^{\text{init}}(X) \cdot \mathcal{T} e^{-i\epsilon \int_0^t \mathbf{V}_{\text{W, MQC}}^l(X, t') dt'/\hbar} \\ &= \langle \mathcal{T} e^{-i\epsilon \int_0^t \mathbf{V}_{\text{W, MQC}}^l(X, t') dt'/\hbar} \rangle_{\rho_{\text{W}}^{\text{init}}(X)}, \end{aligned} \quad (10)$$

where the average in the last row is defined in general as

$$\langle \mathbf{A}(X) \rangle_{\rho(X)} := \frac{\text{Tr}_e \int dX \rho(X) \cdot \mathbf{A}(X)}{\text{Tr}_e \int dX \rho(X)}.$$

Equation (10) makes it clear that the only fundamental difference between the MSDR and IMSDR introduced in Ref. 29 is the time ordering operator \mathcal{T} present in the MSDR but missing in the IMSDR. To gain some insight into effects of approximations made in Eqs. (9) and (10), we may look at the original DR where similar approximations are made. When the propagation uses the average Hamiltonian, the original DR is exact if both Hamiltonians are at most quadratic and if the force constants of quadratic terms in $\hat{\mathbf{H}}^0$ and $\hat{\mathbf{H}}^\epsilon$ are equal. If the force constants differ, DR is able to capture the initial decay of fidelity but not the subsequent recurrences. This failure is due to an approximation equivalent to Eq. (9) because the classical propagation of the Wigner transformed perturbation is exact for quadratic potentials. When higher order terms are present in the Hamiltonians, approximations made in Eqs. (9) and (10) introduce additional inaccuracies. (Some of the problems just mentioned may be reduced by a prefactor correction to the DR recently derived by Zambrano and Ozorio de Almeida.⁵⁷) In comparison with the DR, the situation is more complicated in the case of the MSDR due to couplings between PESs. The method is generally not exact even for quadratic Hamiltonians. On the other hand, the problem of recurrences occurring in the case of the DR for two harmonic oscillators with different frequencies is usually diminished during nonadiabatic dynamics thanks to couplings between PESs.

B. Propagation scheme

Equation (10) gives f_{MSDR} in terms of $\mathbf{V}_{\text{W, MQC}}^l(X, t)$; what remains to be done is finding a prescription for $\mathbf{V}_{\text{W, MQC}}^l(X, t)$. The exact equation of motion for $\mathbf{V}_w^l(X, t)$ in the interaction picture is

$$\frac{\partial \mathbf{V}_w^l(X, t)}{\partial t} = \frac{i}{\hbar} [\hat{\mathbf{H}}^0, \hat{\mathbf{V}}^l(t)]_w(X). \quad (11)$$

Note that Eq. (11) is, up to the sign, the same as the partially Wigner transformed Liouville-Von Neumann equation describing the propagation of the density matrix of the unperturbed system

$$\frac{\partial \rho_w(X, t)}{\partial t} = -\frac{i}{\hbar} [\hat{\mathbf{H}}^0, \hat{\rho}(t)]_w(X). \quad (12)$$

We will take advantage of this analogy and derive our approximate propagation scheme from Eq. (12) instead of from Eq. (11). This will turn out to be slightly easier and, more importantly, we will simultaneously find an approximate solution of a much more general problem of propagating the density matrix. Below we omit superscript 0 in $\hat{\mathbf{H}}^0$ since now

we deal with a single Hamiltonian. In the system consisting of light electrons and heavy nuclei, Eq. (12) is approximated to the first order in the mass ratio $\sqrt{\frac{m}{M}}$ by the mixed quantum-classical Liouville equation^{17,58–63}

$$\frac{\partial \rho_{\text{W,MQC}}}{\partial t} = -\frac{i}{\hbar} [\mathbf{H}_{\text{W}}, \rho_{\text{W,MQC}}] + \frac{1}{2} (\{\mathbf{H}_{\text{W}}, \rho_{\text{W,MQC}}\} - \{\rho_{\text{W,MQC}}, \mathbf{H}_{\text{W}}\}), \quad (13)$$

where the explicit dependence of $\rho_{\text{W,MQC}}$ on time and on the nuclear phase space coordinate X was omitted for clarity.

Equation (10) together with Eq. (13) define the MSDR. Several numerical approaches exist that solve Eq. (13) in terms of “classical” trajectories $X(t)$. However, since trajectory based methods for solving Eq. (13) are still relatively complicated, below we study two variants of MSDR where Eq. (13) is further approximated. The common feature of the two approximations is that all elements of $\rho_{\text{W}}(X, t)$ are propagated using the same PES (which may, nevertheless, differ for different trajectories). The first approximation is based on the locally mean field approximation and turns out to be nothing else than the dynamics of a swarm of trajectories, each of which is propagated with the Ehrenfest dynamics. The second approximation is based on the FSSH dynamics. For simplicity, from now on the subscript MQC is omitted.

1. Locally mean field dynamics

The first approach starts by rewriting $\rho_{\text{W}}(X, t)$ as

$$\rho_{\text{W}}(X, t) = \rho(X, t) \rho_e(X, t), \quad (14)$$

where $\rho(X, t) := \text{Tr}_e \rho_{\text{W}}(X, t)$ is a scalar function of X and t , and $\rho_e(X, t)$ is the “conditional” density matrix with the property $\text{Tr}_e \rho_e(X, t) = 1$ for all X and t . By substituting the still exact ansatz (14) into Eq. (13), one obtains

$$\begin{aligned} \frac{\partial \rho}{\partial t} \rho_e + \rho \frac{\partial \rho_e}{\partial t} = & -\frac{i}{\hbar} \rho [\mathbf{H}_{\text{W}}, \rho_e] + \frac{1}{2} \frac{\partial \rho}{\partial P} \left[\frac{\partial \mathbf{H}_{\text{W}}}{\partial Q}, \rho_e \right]_+ \\ & + \frac{1}{2} \rho \left[\frac{\partial \mathbf{H}_{\text{W}}}{\partial Q}, \frac{\partial \rho_e}{\partial P} \right]_+ - \frac{1}{2} \frac{\partial \rho}{\partial Q} \left[\frac{\partial \mathbf{H}_{\text{W}}}{\partial P}, \rho_e \right]_+ \\ & - \frac{1}{2} \rho \left[\frac{\partial \mathbf{H}_{\text{W}}}{\partial P}, \frac{\partial \rho_e}{\partial Q} \right]_+, \end{aligned} \quad (15)$$

where $[\mathbf{A}, \mathbf{B}]_+ = \mathbf{A} \cdot \mathbf{B} + \mathbf{B} \cdot \mathbf{A}$ is the anticommutator. In the next step, the trace over the electronic degrees of freedom is performed, which in the diabatic basis leads to the following equation of motion for $\rho(X, t)$:

$$\begin{aligned} \frac{\partial \rho}{\partial t} = & \frac{\partial \rho}{\partial P} \left\langle \frac{\partial \mathbf{H}_{\text{W}}}{\partial Q} \right\rangle_e - \frac{\partial \rho}{\partial Q} \left\langle \frac{\partial \mathbf{H}_{\text{W}}}{\partial P} \right\rangle_e \\ & + \rho \text{Tr}_e \left(\frac{\partial \mathbf{H}_{\text{W}}}{\partial Q} \cdot \frac{\partial \rho_e}{\partial P} \right), \end{aligned} \quad (16)$$

where $\langle \mathbf{A} \rangle_e = \text{Tr}_e(\rho_e \cdot \mathbf{A})$ is a partial average of \mathbf{A} over the electronic subspace and where we have used that $\text{Tr}_e(\frac{\partial \mathbf{H}_{\text{W}}}{\partial P} \cdot \frac{\partial \rho_e}{\partial Q}) = \frac{P}{M} \text{Tr}_e(\frac{\partial \rho_e}{\partial Q}) = 0$. (The equation of motion in the adiabatic basis will be derived later.) Substitution of Eq. (16) back

into Eq. (15) yields

$$\begin{aligned} \rho \frac{\partial \rho_e}{\partial t} = & -\frac{i}{\hbar} \rho [\mathbf{H}_{\text{W}}, \rho_e] \\ & + \frac{\partial \rho}{\partial P} \left(\frac{1}{2} \left[\frac{\partial \mathbf{H}_{\text{W}}}{\partial Q}, \rho_e \right]_+ - \left\langle \frac{\partial \mathbf{H}_{\text{W}}}{\partial Q} \right\rangle_e \cdot \rho_e \right) \\ & + \frac{1}{2} \rho \left[\frac{\partial \mathbf{H}_{\text{W}}}{\partial Q}, \frac{\partial \rho_e}{\partial P} \right]_+ \\ & - \frac{\partial \rho}{\partial Q} \left(\frac{1}{2} \left[\frac{\partial \mathbf{H}_{\text{W}}}{\partial P}, \rho_e \right]_+ - \left\langle \frac{\partial \mathbf{H}_{\text{W}}}{\partial P} \right\rangle_e \cdot \rho_e \right) \\ & - \rho \left\langle \frac{\partial \mathbf{H}_{\text{W}}}{\partial P} \right\rangle_e \cdot \frac{\partial \rho_e}{\partial Q} - \rho \rho_e \text{Tr} \left(\frac{\partial \mathbf{H}_{\text{W}}}{\partial Q} \cdot \frac{\partial \rho_e}{\partial P} \right), \end{aligned} \quad (17)$$

where identity $\frac{1}{2} \left[\frac{\partial \mathbf{H}_{\text{W}}}{\partial P}, \frac{\partial \rho_e}{\partial Q} \right]_+ = \frac{P}{M} \frac{\partial \rho_e}{\partial Q} = \left\langle \frac{\partial \mathbf{H}_{\text{W}}}{\partial P} \right\rangle_e \cdot \frac{\partial \rho_e}{\partial Q}$ was used in the fifth row. Both Eqs. (16) and (17) contain terms of the form $\left\langle \frac{\partial \mathbf{H}_{\text{W}}}{\partial P} \right\rangle_e \frac{\partial f}{\partial Q}$ and $\left\langle \frac{\partial \mathbf{H}_{\text{W}}}{\partial Q} \right\rangle_e \frac{\partial f}{\partial P}$, which can be combined with the time derivative $\frac{\partial f}{\partial t}$ to form the convective derivative

$$\frac{Df}{Dt} = \frac{\partial f}{\partial t} + \dot{Q} \frac{\partial f}{\partial Q} + \dot{P} \frac{\partial f}{\partial P}$$

and transform the equations from the Eulerian reference frame at rest to the Lagrangian reference frame moving with the phase space flow given by the vector field

$$(\dot{Q}, \dot{P}) = \left(\left\langle \frac{\partial \mathbf{H}_{\text{W}}}{\partial P} \right\rangle_e, -\left\langle \frac{\partial \mathbf{H}_{\text{W}}}{\partial Q} \right\rangle_e \right). \quad (18)$$

In the Lagrangian frame, Eq. (16) transforms to

$$\frac{D\rho}{Dt} = \rho \text{Tr}_e \left(\frac{\partial \mathbf{H}_{\text{W}}}{\partial Q} \cdot \frac{\partial \rho_e}{\partial P} \right). \quad (19)$$

Since the two terms in the fourth row of Eq. (17) cancel each other exactly, this equation transforms to

$$\begin{aligned} \frac{D\rho_e}{Dt} = & -\frac{i}{\hbar} [\mathbf{H}_{\text{W}}, \rho_e] \\ & + \frac{1}{\rho} \frac{\partial \rho}{\partial P} \left(\frac{1}{2} \left[\frac{\partial \mathbf{H}_{\text{W}}}{\partial Q}, \rho_e \right]_+ - \left\langle \frac{\partial \mathbf{H}_{\text{W}}}{\partial Q} \right\rangle_e \cdot \rho_e \right) \\ & + \left(\frac{1}{2} \left[\frac{\partial \mathbf{H}_{\text{W}}}{\partial Q}, \frac{\partial \rho_e}{\partial P} \right]_+ - \left\langle \frac{\partial \mathbf{H}_{\text{W}}}{\partial Q} \right\rangle_e \cdot \frac{\partial \rho_e}{\partial P} \right) \\ & - \rho_e \text{Tr}_e \left(\frac{\partial \mathbf{H}_{\text{W}}}{\partial Q} \cdot \frac{\partial \rho_e}{\partial P} \right). \end{aligned} \quad (20)$$

Note that the second and third rows of the right-hand side of Eq. (20) contain differences (put in parentheses for emphasis) between products of the electronic density matrix (or its P derivative) with the nonaveraged and averaged gradients of the Hamiltonian. Therefore, the second and third rows equal to zero when the Hamiltonian is uncoupled and occupied surfaces have equal gradients, when the Hamiltonian is uncoupled and only one surface is occupied, or when $\partial \rho / \partial p$ and $\partial \rho_e / \partial p$ vanish. In situations where these conditions are satisfied at least approximately, the second and third rows will be small compared to the first and fourth rows of Eq. (20). Another situation in which the second and third rows may be less important is the limit of strong coupling that effectively averages the Hamiltonian. The last term on the right-hand side of

Eq. (20) corresponds to the right-hand side of Eq. (19) and is responsible for maintaining $\text{Tr}_e \rho_e(X, t) = 1$ during the (non-approximated) MQC dynamics.

Until now all operations have been exact and Eqs. (19) and (20) are equivalent to the original mixed quantum classical Liouville equation (13). Now we will make the locally mean field approximation: Specifically, once in the Lagrangian reference frame, all terms in both Eqs. (19) and (20) containing phase space derivatives of $\rho(X, t)$ or $\rho_e(X, t)$ are neglected to obtain the approximate locally mean-field equations of motion. The resulting equation for $\rho(X, t)$ in the Lagrangian reference frame is simply

$$\frac{D\rho_{\text{LMFD}}}{Dt} = 0, \quad (21)$$

and the equation of motion for the electronic part of the density matrix $\rho_e(X, t)$ is

$$\frac{D\rho_{e,\text{LMFD}}}{Dt} = -\frac{i}{\hbar} [\mathbf{H}_W, \rho_{e,\text{LMFD}}]. \quad (22)$$

Both equations can be combined together and transformed back to the Eulerian reference frame to yield the equation of motion for the total density matrix $\rho_W(X, t)$,

$$\begin{aligned} \frac{\partial \rho_{W,\text{LMFD}}}{\partial t} = & -\frac{i}{\hbar} [\mathbf{H}_W, \rho_{W,\text{LMFD}}] \\ & + \frac{\partial \rho_{W,\text{LMFD}}}{\partial P} \left\langle \frac{\partial \mathbf{H}_W}{\partial Q} \right\rangle_e - \frac{\partial \rho_{W,\text{LMFD}}}{\partial Q} \frac{P}{M}, \end{aligned} \quad (23)$$

where we have used that $\langle \frac{\partial \mathbf{H}_W}{\partial P} \rangle_e = \frac{P}{M}$.

We call the dynamics expressed by Eq. (23) [or, equivalently, by Eqs. (18), (21), and (22)] the *locally mean field dynamics* (LMFD) since the force acting on nuclei at position X is the force averaged over the “electronic” part of the density matrix $\rho_e(X, t)$ at X . Note that the well-known *Ehrenfest dynamics* (which uses a single nuclear trajectory) can be derived in a similar way using an approximate ansatz $\rho_W^{\text{ED}} = \delta(X - X(t))\rho_e(t)$, where δ is the Dirac delta distribution and $X(t)$ is the phase space coordinate at time t .⁶⁴ Similarly, a truly *mean field dynamics* for a wavepacket different from a δ distribution can be derived using an (again approximate) ansatz in the form of a Hartree product $\rho_W^{\text{MFD}}(X, t) = \rho(X, t)\rho_e(t)$.

As can be seen from Eq. (23), for pure states, each phase space point is propagated by the mean field Ehrenfest dynamics, according to Eq. (18). Nevertheless, in contrast to the purely mean field dynamics, Eq. (23) describes the propagation of the density $\rho_W(X, t)$ using different values of $\langle \frac{\partial \mathbf{H}_W}{\partial Q} \rangle_e$ and $\langle \frac{\partial \mathbf{H}_W}{\partial P} \rangle_e$ for each value of X . Interestingly, this dynamics corresponds exactly to the nuclear dynamics appearing in the nonadiabatic initial value representation model,^{14,65} which uses the Meyer-Miller-Stock-Thoss Hamiltonian.^{66,67} Also note that outside of coupling regions, when only one surface is occupied, resulting trajectories are equivalent to those obtained with the Born-Oppenheimer dynamics.

To derive a corresponding LMFD equation of motion in the adiabatic basis, one can express the mixed quantum classical Liouville equation (13) in the adiabatic basis,¹⁷ use the exact ansatz (14), and apply a similar LMFD approximation

as above. However, this procedure is quite tedious in the adiabatic basis. The LMFD in adiabatic basis can be obtained more easily by directly transforming the final LMFD equation of motion [Eq. (21)] from diabatic to adiabatic basis using the relations¹⁷

$$\left(\frac{\partial \mathbf{A}_W}{\partial Q} \right)^A = \frac{\partial \mathbf{A}_W^A}{\partial Q} - [\mathbf{A}_W^A, \mathbf{F}] \quad \text{and} \quad (24)$$

$$\left(\frac{\partial \mathbf{A}_W}{\partial P} \right)^A = \frac{\partial \mathbf{A}_W^A}{\partial P}, \quad (25)$$

where the superscript A denotes the transformation to the adiabatic basis, and \mathbf{F} is the vector matrix of nonadiabatic coupling vectors. Specifically, $\mathbf{A}_W^A(X, t)$ is a matrix obtained by first partially Wigner transforming a general operator $\hat{\mathbf{A}}(t)$ [to form $\mathbf{A}_W(X, t)$] and then by transforming $\mathbf{A}_W(X, t)$ into the adiabatic basis. Matrix \mathbf{F} is defined componentwise by $F_{jk}(Q) = \langle \alpha_j(Q) | \frac{\partial}{\partial Q} \alpha_k(Q) \rangle$, where $|\alpha_k(Q)\rangle$ is k th element of the adiabatic basis at position Q . Applying relations (24) and (25) to derivatives of both \mathbf{H}_W and $\rho_{W,\text{LMFD}}$ in Eq. (23) immediately yields the LMFD equation of motion in the adiabatic basis,

$$\begin{aligned} \frac{\partial \rho_{W,\text{LMFD}}^A}{\partial t} = & -\frac{i}{\hbar} \left[\mathbf{H}_W^A(X) - i\hbar \frac{P}{M} \mathbf{F}(Q), \rho_{W,\text{LMFD}}^A \right] \\ & + \frac{\partial \rho_{W,\text{LMFD}}^A}{\partial P} \cdot \left(\left\langle \frac{\partial \mathbf{H}_W^A}{\partial Q} \right\rangle_e - \langle [\mathbf{H}_W^A, \mathbf{F}] \rangle_e \right) \\ & - \frac{\partial \rho_{W,\text{LMFD}}^A}{\partial Q} \frac{P}{M}, \end{aligned} \quad (26)$$

where \mathbf{H}_W^A is the diabatic Hamiltonian matrix \mathbf{H}_W expressed in the adiabatic basis. Note that \mathbf{H}_W^A consists only of the kinetic energy term and the diagonal adiabatic potential energy matrix; in particular, \mathbf{H}_W^A does not contain the nonadiabatic couplings. Again, the dynamics of a single trajectory is identical to the Ehrenfest dynamics.

2. Fewest switches surface hopping

The second alternative approximate propagation scheme is based on the physically motivated FSSH algorithm.²⁵ In this scheme, each phase space point representing the Wigner density distribution is propagated independently using the FSSH dynamics. Compared to the LMFD, the FSSH is used at no additional cost, except for the stochastic hopping algorithm itself, because the same Eq. (22) (or its equivalent in the adiabatic basis) has to be solved during the electronic part of the dynamics. On the other hand, averaging the force over electronic states is avoided in the FSSH. Still, approximate nature of the FSSH algorithm may lead to inaccuracies in certain situations. The well-known problem is the “overcoherence” of the dynamics, which is essentially caused by the fact that all elements of the density matrix propagate on the same PES (which may change during the propagation). This may lead to unphysical density matrix elements and to inconsistency with PES occupation numbers. In such situations, the MSDR will be also negatively affected, even though the problem is often mitigated because the FSSH is only used to compute

the fidelity and not the dynamics itself. In other words, error cancellations are expected. As will be shown below, neither LMFD nor FSSH is universally optimal and the best propagation method depends on the problem studied.

C. Algorithm

1. General initial state

To compute $f_{\text{MSDR}}(t)$, we rewrite the initial density matrix exactly in the form

$$\rho_{\text{W}}^{\text{init}}(X) = \rho^{\text{init}}(X) \rho_e^{\text{init}}(X), \quad (27)$$

where $\rho^{\text{init}}(X) := \text{Tr}_e \rho_{\text{W}}^{\text{init}}(X)$. Scalar nuclear density $\rho^{\text{init}}(X)$ is sampled by N_{traj} phase space points that serve as initial conditions for N_{traj} trajectories propagated using either the LMFD or FSSH dynamics. For each generated phase space point, the electronic part $\rho_e^{\text{init}}(X)$ satisfies $\text{Tr}_e \rho_e^{\text{init}}(X) = 1$. In the case of LMFD, X determines the initial condition completely. In the case of FSSH, one also needs to select the initial surface randomly for each trajectory according to the following prescription: For a trajectory starting at X , the probability for its initial surface to be surface j is given by the diagonal element $\rho_{e,j}^{\text{init}}(X)$. Equation (10) for fidelity amplitude is rewritten as

$$f_{\text{MSDR}}(t) = \langle \text{Tr}_e [\rho_e^{\text{init}}(X) \cdot \mathcal{T} e^{-i\epsilon \int_0^t \mathbf{V}_{\text{W}}^{\text{l}}(X,t') dt' / \hbar}] \rangle_{\rho^{\text{init}}(X)}, \quad (28)$$

where we have used the notation

$$\langle A(X) \rangle_{\rho(X)} := \frac{\int dX \rho(X) A(X)}{\int dX \rho(X)}$$

and the fact that $\langle \text{Tr}_e \rho_e^{\text{init}}(X) \rangle_{\rho^{\text{init}}(X)} = 1$. The time-ordered product $\mathcal{T} e^{-i\epsilon \int_0^t \mathbf{V}_{\text{W}}^{\text{l}}(X,t') dt' / \hbar}$ is evaluated along each trajectory by successive multiplication of short time propagators corresponding to each time step. The exponent of each short time propagator is computed using

$$\mathbf{V}_{\text{W}}^{\text{l}}(X, t) = \mathbf{U}^0(X, t)^{-1} \cdot \mathbf{V}_{\text{W}}(X^0(t)) \cdot \mathbf{U}^0(X, t), \quad (29)$$

where

$$\mathbf{U}^0(X, t) = \mathcal{T} e^{-i \int_0^t \mathbf{H}_{\text{W}}^0(X^0(t')) dt' / \hbar}, \quad (30)$$

and $X^0(t)$ denotes a trajectory of \mathbf{H}_{W}^0 starting at $X^0(0) = X$. Equation (29) can be vaguely interpreted as a combination of a quantum interaction picture for the electrons and a ‘‘classical interaction picture’’ (in which the perturbation is neglected) for the nuclei. Operator $\mathbf{U}^0(X, t)$ is again computed by successive multiplication of short time propagators along the trajectory. At the end of the dynamics, the weighted phase space average in Eq. (28) is computed as the arithmetic average over all trajectories

$$f_{\text{MSDR}}(t) = \frac{1}{N_{\text{traj}}} \sum_{N=1}^{N_{\text{traj}}} \text{Tr}_e \left[\rho_e^{\text{init}}(X_N) \cdot \mathcal{T} \prod_{M=1}^{M_{\text{step}}} e^{-i\epsilon \mathbf{V}_{\text{W}}^{\text{l}}(X_N, M\Delta t) \Delta t / \hbar} \right]. \quad (31)$$

2. Initial Hartree product state

The algorithm simplifies slightly when the initial density operator $\hat{\rho}^{\text{init}}$ is a Hartree product

$$\hat{\rho}^{\text{init}} = \hat{\rho}_{\text{N}}^{\text{init}} \otimes \rho_e^{\text{init}}, \quad (32)$$

where $\hat{\rho}_{\text{N}}^{\text{init}}$ and ρ_e^{init} are the nuclear and electronic density operators, respectively. This Hartree approximation is usually an excellent approximation outside of coupling regions when only one PES is occupied. For initial density in the product form (32), $\rho_{\text{W}}^{\text{init}}(X) = \rho^{\text{init}}(X) \rho_e^{\text{init}}$, where $\rho^{\text{init}}(X) = [\rho_{\text{N}}^{\text{init}}]_{\text{W}}(X)$ and ρ_e^{init} is independent of X . Equations (28) and (31) become

$$f_{\text{MSDR}}(t) = \text{Tr}_e [\rho_e^{\text{init}} \cdot \langle \mathcal{T} e^{-i\epsilon \int_0^t \mathbf{V}_{\text{W}}^{\text{l}}(X,t') dt' / \hbar} \rangle_{\rho^{\text{init}}(X)}] \quad (33)$$

and

$$f_{\text{MSDR}}(t) = \text{Tr}_e \left[\rho_e^{\text{init}} \cdot \frac{1}{N_{\text{traj}}} \sum_{N=1}^{N_{\text{traj}}} \mathcal{T} \prod_{M=1}^{M_{\text{step}}} e^{-i\epsilon \mathbf{V}_{\text{W}}^{\text{l}}(X_N, M\Delta t) \Delta t / \hbar} \right]. \quad (34)$$

3. ‘‘Electronically pure’’ initial state

The algorithm simplifies also for ‘‘electronically pure’’ initial states, by which we mean (in the most general sense) states for which the electronic density matrix $\rho_e^{\text{init}}(X)$ in the product (27) is pure for all X , i.e., satisfies the condition $\text{Tr}_e [\rho_e^{\text{init}}(X)^2] = 1$ and can be written as the tensor product

$$\rho_e^{\text{init}}(X) = \mathbf{c}^{\text{init}}(X) \otimes \mathbf{c}^{\text{init}}(X)^\dagger \quad (35)$$

in terms of an initial electronic wavefunction $\mathbf{c}^{\text{init}}(X)$. The generalized electronically pure states include, as a special case, the Hartree product (32) in which the constant electronic matrix ρ_e^{init} is pure (while the nuclear factor $\hat{\rho}_{\text{N}}^{\text{init}}$ may be mixed). To derive the simplified expression for $f_{\text{MSDR}}(t)$, we first rewrite the approximate Wigner transform of the echo operator in Eq. (28) as a product of the electronic evolution operators

$$\mathcal{T} e^{-i\epsilon \int_0^t \mathbf{V}_{\text{W}}^{\text{l}}(X,t') dt' / \hbar} = \mathbf{U}^0(X, t)^{-1} \cdot \mathbf{U}^\epsilon(X, t), \quad (36)$$

where $\mathbf{U}^0(X, t)$ was defined in Eq. (30) and, similarly,

$$\mathbf{U}^\epsilon(X, t) = \mathcal{T} e^{-i \int_0^t \mathbf{H}_{\text{W}}^{\text{l}}(X^0(t')) dt' / \hbar}. \quad (37)$$

Note that the electronic evolution operators $\mathbf{U}^0(X, t)$ and $\mathbf{U}^\epsilon(X, t)$ are defined separately for each nuclear trajectory. Using expression (36), we can rewrite the MSDR of fidelity amplitude (28) as

$$f_{\text{MSDR}}(t) = \langle \text{Tr}_e [\rho_e^{\text{init}}(X) \cdot \mathbf{U}^0(X, t)^{-1} \cdot \mathbf{U}^\epsilon(X, t)] \rangle_{\rho^{\text{init}}(X)}. \quad (38)$$

This expression, which is still valid for any initial state, is equivalent to Eq. (28) when either the LMFD or FSSH dynamics is used for propagation.

For electronically pure states (35), Eq. (38) further simplifies into the weighted phase space average

$$f_{\text{MSDR}}(t) = \langle \mathbf{c}^0(X, t)^\dagger \cdot \mathbf{c}^\epsilon(X, t) \rangle_{\rho^{\text{init}}(X)}, \quad (39)$$

where $\mathbf{c}^\epsilon(X, t)$ is the wavefunction with initial condition $\mathbf{c}^\epsilon(X, 0) = \mathbf{c}^{\text{init}}(X)$ that solves the Schrödinger equation $\frac{\partial \mathbf{c}^\epsilon(X, t)}{\partial t} = -\frac{i}{\hbar} \mathbf{H}_W^\epsilon(X^0(t)) \cdot \mathbf{c}^\epsilon(X, t)$ for a single discrete electronic degree of freedom in the Lagrangian reference frame given by \mathbf{H}_W^0 . In both propagation algorithms currently used with the MSDR, i.e., the LMFD and FSSH dynamics, $\mathbf{c}^0(X, t)$ is already available; only $\mathbf{c}^\epsilon(X, t)$ has to be determined additionally. Expressed explicitly in terms of trajectories, Eq. (39) allows computing the fidelity amplitude simply as

$$f_{\text{MSDR}}(t) = \frac{1}{N_{\text{traj}}} \sum_{N=1}^{N_{\text{traj}}} \mathbf{c}_N^0(X, t)^\dagger \cdot \mathbf{c}_N^\epsilon(X, t), \quad (40)$$

where both $\mathbf{c}_N^0(X, t)$ and $\mathbf{c}_N^\epsilon(X, t)$ are computed using the same trajectories propagated with the Hamiltonian \mathbf{H}_W^0 .

III. RESULTS

To test the MSDR, we considered several model systems allowing comparison with the exact quantum-mechanical solution in both the adiabatic and diabatic bases. Specifically, we used variants of the three one-dimensional model potentials introduced by Tully²⁵ and the simple two-level model of photodissociation of NaI.^{68–70} The mass in Tully's models was set to 2000 a.u., approximately corresponding to the mass of the hydrogen atom. The reduced mass in the model of photodissociation of NaI was set to 35480.25 a.u.

The initial density matrix was in all cases a density matrix of a pure state, so f_{MSDR} was evaluated using Eq. (40). In Subsections III A and III B, fidelity is used as a quantitative measure of the importance of the nonadiabatic or diabatic couplings on the dynamics. In other words, Hamiltonian $\hat{\mathbf{H}}^0$ is the diagonal adiabatic (Subsection III A) or diabatic (Subsection III B) Hamiltonian and Hamiltonian $\hat{\mathbf{H}}^\epsilon$ is the full nonadiabatic (Subsec. III A) or nonadiabatic (Subsec. III B) Hamiltonian, respectively. If not mentioned otherwise, the dynamics on $\hat{\mathbf{H}}^0$ uses the LMFD algorithm. Since the PESs of $\hat{\mathbf{H}}^0$ are decoupled and (with one exception shown in Fig. 2) only one PES is occupied initially, the dynamics reduces to the simpler Born-Oppenheimer classical dynamics of an ensemble of phase space points.

A. Nonadiabaticity of quantum dynamics

In this subsection, the fidelity criterion of nonadiabaticity of the quantum dynamics in the adiabatic basis is studied together with the MSDR approximation of fidelity. The IMSDR approximation is not studied in detail since it fails completely in the adiabatic case. This can be seen in Figure 2(a), which shows results for the photodissociation dynamics of NaI close to the adiabatic limit. A low energy wavepacket oscillates on the excited adiabatic PES, crossing the coupling region twice per period, each time losing a bit of the excited PES population due to the transition to the ground PES. The MSDR reproduces the associated fidelity decay very well. Both the

survival probability (P_{QM}) and the approximate MSDR trace the decaying fidelity (F_{QM}) fairly closely. Using the same system and a wavepacket with a higher initial energy, Fig. 2(b) shows that the MSDR often retains its accuracy even far from the adiabatic limit. Nevertheless, special care should be taken in such cases.

In both examples discussed above, only one PES was occupied initially. Yet the MSDR works also with more general initial conditions, as shown in Fig. 2(c) using Tully's single avoided crossing model. Here 75% of the initial density is located on the lower PES, and the rest on the upper one. Note that when more than one PES of $\hat{\mathbf{H}}^0$ is occupied, one must watch out for the intrinsic deficiencies of the underlying dynamical methods. If the LMFD is used for propagation (not shown), each trajectory propagates on an average PES, given by the weighted average of all occupied PES, even outside of coupling regions. When the FSSH based algorithm is used [as shown in Fig. 2(c)], other problems may occur in a similar situation, i.e., when wavepacket dynamics on the lower and upper PESs differ substantially outside of coupling regions. In the case shown, the MSDR works very well with both the LMFD and FSSH dynamics and the results of the two approaches are almost indistinguishable. In addition, Fig. 2(c) demonstrates the convergence of the MSDR with the number of trajectories showing that as few as 16 trajectories suffice for a relatively accurate approximation of F_{QM} . In the case of the DR (Refs. 40 and 53) and IMSDR,²⁹ exact formulas exist for the number of required trajectories as a function of fidelity and the statistical error. Such an exact formula has not been derived for the MSDR, but—as for the DR and IMSDR—more trajectories are needed to simulate lower fidelity.

B. Nonadiabaticity of quantum dynamics

In this subsection, the fidelity criterion of nonadiabaticity of the quantum dynamics in the diabatic basis is studied together with the IMSDR and MSDR approximations of fidelity. The IMSDR was already shown to perform well only when the dynamics was close to the diabatic limit.²⁹ As demonstrated here, the MSDR performs better and works well for a broader range of problems and for lower wavepacket energies. Comparisons of both methods with numerically exact quantum fidelity (F_{QM}) in the diabatic basis can be found in Fig. 3. In most cases when the dynamics is fairly close to the diabatic limit (not shown) both extensions of the DR work very well and F_{MSDR} is often almost indistinguishable from F_{QM} . Figure 3(a) demonstrates, on the extended coupling model of Tully,²⁵ that the survival probability P_{QM} itself is not always a good indicator of nonadiabaticity of the dynamics. Here, F_{QM} decays quickly to zero despite P_{QM} staying close to unity. Indeed, the quantum dynamics on $\hat{\mathbf{H}}^0$ and $\hat{\mathbf{H}}^\epsilon$ are very different. Both extensions of the DR reproduce the decay of F_{QM} very accurately, even though the good performance of the IMSDR should be considered rather accidental. Using the double avoided crossing model of Tully,²⁵ Fig. 3(b) shows that in many cases, the MSDR can accurately reproduce complicated fidelity behavior far from the diabatic limit. Not surprisingly, the IMSDR method fails here. For comparison, Fig. 3(b) also shows two MSDR results obtained by

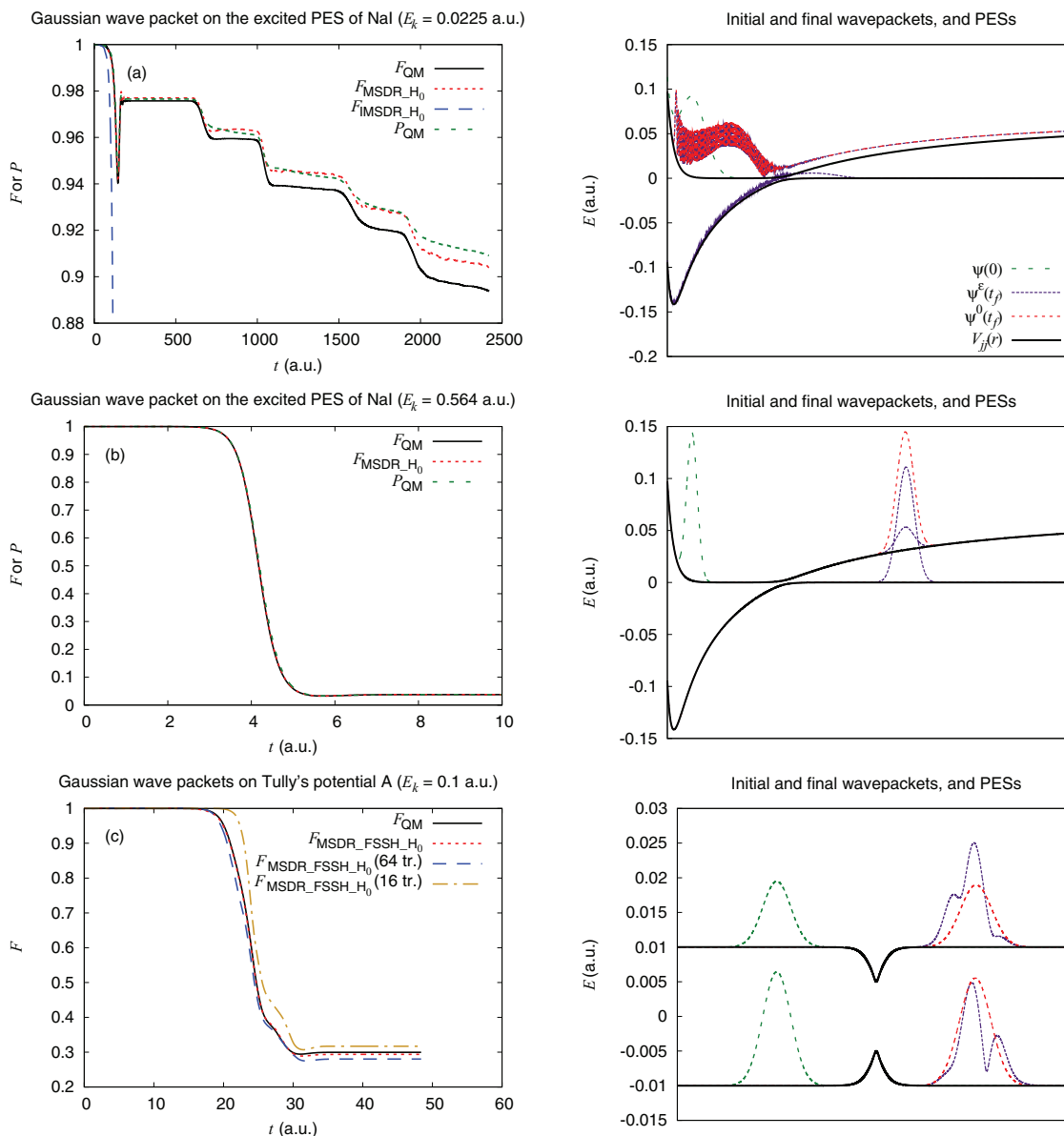


FIG. 2. Nonadiabaticity of quantum dynamics. Panels (a)-(c) compare the numerically exact quantum fidelity (F_{QM}) with the extensions of the DR in the adiabatic basis and (when applicable) with the quantum survival probability (P_{QM}). (a) Dynamics close to the adiabatic limit. (b) Dynamics very far from the adiabatic limit. (c) A more general initial condition with both PESs initially occupied (75% of the initial density on the lower PES, 25% on the upper PES). The convergence of MSDR is shown as well. The panels on the right show corresponding adiabatic PESs $V_{jj}(r)$ as well as initial $[\psi(0)]$ and final $[\psi^0(t_f)]$ and $[\psi^\epsilon(t_f)]$ wavefunctions evolved with \hat{H}^0 and \hat{H}^ϵ , respectively.

exchanging the roles of \hat{H}^0 and \hat{H}^ϵ . Since, in contrast to \hat{H}^0 , \hat{H}^ϵ is coupled, both the LMFD and FSSH dynamics allow transitions between PESs: both are good approximations of F_{QM} . Finally, Fig. 3(c) demonstrates that because the MSDR is a semiclassical method based on classical trajectories, not permitting tunneling, the method has to be applied with care. In the case shown, far from the diabatic limit, the wavepacket on \hat{H}^0 reflects back from the coupling region. In the MSDR, this reflection results in “rephasing” of the trajectories leading to the rise of fidelity back to values close to unity, in disagreement with the quantum result. Even if roles of \hat{H}^0 and \hat{H}^ϵ are exchanged, problems persist. In the quantum dynamics, a major part of the wavepacket on the coupled Hamiltonian \hat{H}^ϵ passes through the coupling region with the aid of diabatic couplings. When the LMFD is used with MSDR, this

behavior and associated fidelity decay are captured qualitatively. When the FSSH dynamics is used, the dynamics is exactly identical to the dynamics on the uncoupled Hamiltonian \hat{H}^0 because all hops in the FSSH algorithm are frustrated. This points out the importance of tunneling in this relatively narrow region of wavepacket energies. When the initial kinetic energy is smaller than that shown in Fig. 3(c), most of the wavepacket bounces back even during quantum dynamics on \hat{H}^ϵ and the MSDR fidelity approaches the quantum result. When the energy is somewhat higher, more trajectories pass the barrier (or fewer hops in the FSSH algorithm on \hat{H}^ϵ are frustrated) and as a consequence the MSDR approaches again the quantum result. Note that the relatively good result of the IMSDR is accidental since the method is not expected to work well so far from the diabatic limit.

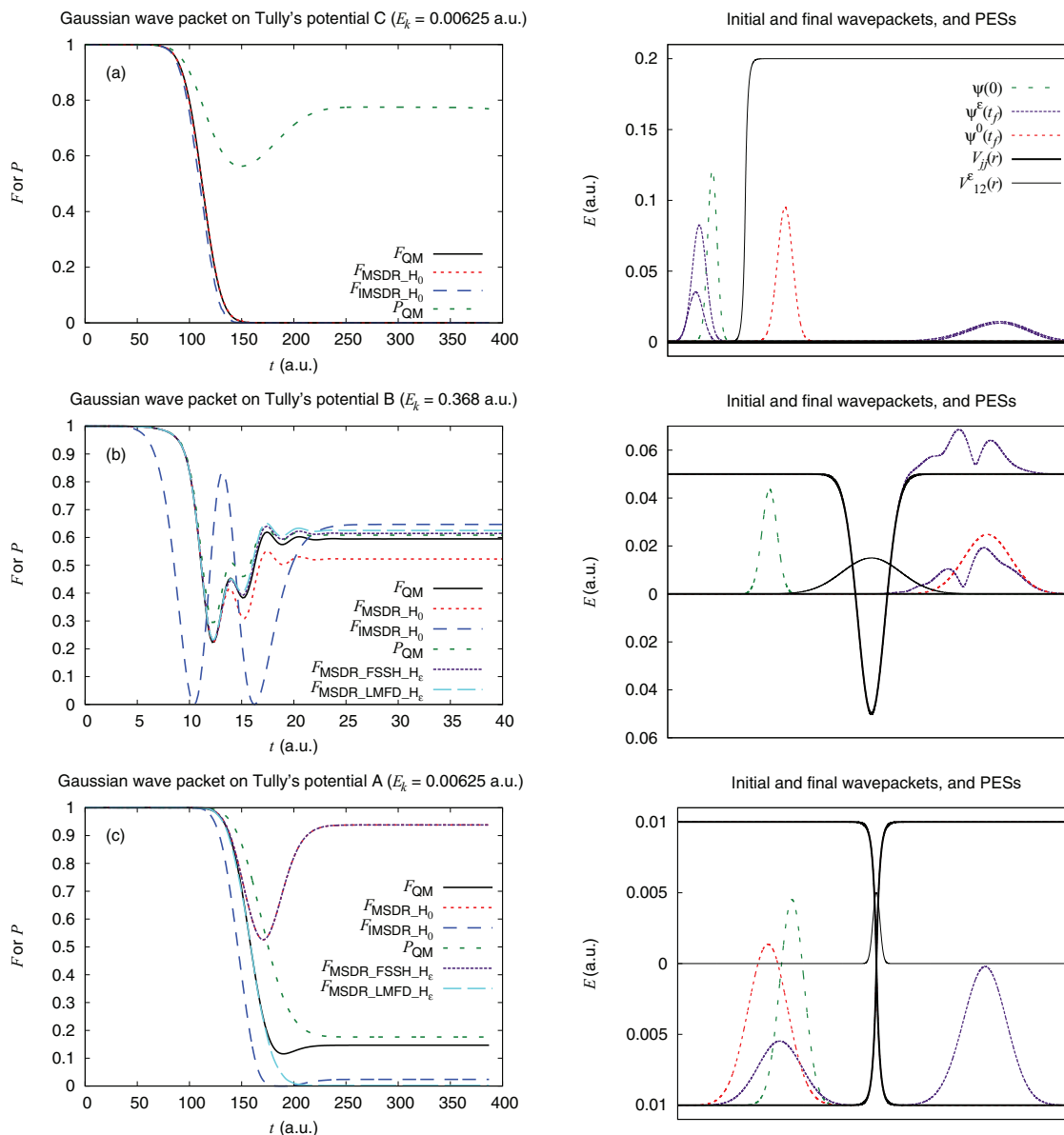


FIG. 3. Nonadiabaticity of quantum dynamics. Panels (a)–(c) compare the numerically exact quantum fidelity (F_{QM}) with extensions of the DR in the diabatic basis and with the quantum survival probability (P_{QM}). (a) Dynamics very far from the diabatic limit. (b) Dynamics in the intermediate range. (c) Dynamics in the region where quantum tunneling is important. The panels on the right show corresponding diabatic PESs $V_{ij}(r)$, diabatic couplings V_{12}^ϵ as well as initial [$\psi(0)$] and final [$\psi^0(t_f)$ and $\psi^\epsilon(t_f)$] wavefunctions evolved with \hat{H}^0 and \hat{H}^ϵ , respectively.

C. Computational details

All quantum calculations in the diabatic basis set were performed using the second order split-operator algorithm.⁷¹ Calculations in the adiabatic basis were done either by transforming the quantum state into the diabatic basis, propagating there, and transforming back into the adiabatic basis, or directly with the second order Fourier method.⁷² The LMFD and FSSH dynamics were done using the second order symplectic Verlet integrator.⁷³

IV. DISCUSSION AND CONCLUSIONS

Results presented above demonstrate that quantum fidelity is useful as a quantitative measure of nonadiabaticity of quantum dynamics. Apart from our work, the fidelity criterion

of nonadiabaticity was, very recently, used to find the optimal time-dependent Hamiltonian maximizing the adiabaticity of the dynamics from an initial state to a desired target state.⁷⁴

As for the MSDR, a semiclassical approximation developed in the present paper, it has proven to be a reliable yet very efficient substitute for the expensive exact quantum dynamics calculation of fidelity. The MSDR is a generalization of DR to nonadiabatic dynamics and may also be used in the diabatic basis set. In addition to quantum effects originating from the interaction of nuclei with electrons, which are included in most mixed quantum-classical methods, the MSDR includes also quantum effects originating from the interference between mixed quantum-classical trajectories representing the evolution of the initial density matrix. Two approximate variants of the MSDR were developed and studied numerically: the former uses the LMFD, derived here,

while the latter employs the FSSH dynamics. The LMFD, although obtained in a different way, is equivalent to the nuclear dynamics appearing in the nonadiabatic initial value representation,^{14,65,75} which is, in turn, nothing else than the Ehrenfest dynamics applied separately to each classical phase space point representing the initial density matrix. Both FSSH and the Ehrenfest method are relatively simple and often used, thus both variants of MSDR can be easily implemented into any FSSH or Ehrenfest dynamics code, especially for pure states.

In Sec. III, we have demonstrated that for one-dimensional model systems the MSDR often works satisfactorily even far from the adiabatic or diabatic limit. The method has yet to be tested in multi-dimensional systems. Nevertheless, results obtained with the original Born-Oppenheimer DR demonstrate that the convergence of the method is actually independent of the dimensionality of a problem⁵³ and that the accuracy does not deteriorate with dimensionality.⁷⁶ Thus, we expect that the MSDR would perform well especially in chaotic multi-dimensional systems such as some molecules, provided that the underlying mixed quantum-classical dynamics is a reasonable approximation to the quantum dynamics. Unfortunately, this is not always the case. It is well known that the Ehrenfest dynamics (and also the LMFD) can be qualitatively incorrect when coupling vanishes after passing a coupling region and more PESs are occupied. In the MSDR, this problem is often less significant, because in many cases after passing the coupling region fidelity does not decay anymore. The FSSH dynamics also suffers from several problems besides the inaccuracies caused by the classical description of nuclei, such as the problem of “excessive coherence” related (similarly as for the LMFD) to the fact that all matrix elements of the density matrix attached to a trajectory evolve on the same PES. In many cases, this can be alleviated by applying the “decoherence” correction.^{77–81} Including a similar correction into the MSDR method should be straightforward and will be explored in future work. Another possibility how to overcome some deficiencies of the LMFD or FSSH dynamics would be to use the MSDR together with one of the propagation methods attempting to solve the mixed quantum-classical Liouville equation directly.

When the underlying propagation scheme is sufficiently accurate, the MSDR provides an efficient approximation to the rigorous quantitative measure of nonadiabaticity or nonadiabaticity of the dynamics based on quantum fidelity. As a result, the MSDR may be used to decide—before running the quantum dynamics itself—which PESs or Hamiltonian terms are important. Due to the generality of definition (1), fidelity and the MSDR approximation can be employed in many other applications with nonadiabatic dynamics, depending on the choice of \hat{H}^0 and \hat{H}^ϵ . An example would be the evaluation of the importance of additional terms in a nonadiabatic Hamiltonian including spin-orbit coupling terms or couplings to an external field. In this case, both \hat{H}^0 and \hat{H}^ϵ are coupled by nonadiabatic coupling terms, and the additional term of interest, missing in \hat{H}^0 , is present in \hat{H}^ϵ . Alternatively, F_{QM} may be used to evaluate quantitatively the accuracy of the quantum dynamics with an approximate or interpolated nonadiabatic Hamiltonian \hat{H}^0 in comparison with the quantum dynamics

with an accurate nonadiabatic Hamiltonian \hat{H}^ϵ . This application would be a generalization to nonadiabatic dynamics of the idea proposed for adiabatic dynamics in Refs. 76 and 82. Finally, the MSDR could be used, in principle, to compute all quantities expressible in terms of quantum fidelity or quantum fidelity amplitude, such as various nonadiabatic spectra.

ACKNOWLEDGMENTS

This research was supported by the Swiss NSF NCCR MUST (Molecular Ultrafast Science & Technology) and by the EPFL.

- ¹L. J. Butler, *Annu. Rev. Phys. Chem.* **49**, 125 (1998).
- ²G. A. Worth and L. S. Cederbaum, *Annu. Rev. Phys. Chem.* **55**, 127 (2004).
- ³*Non-Adiabatic Effects in Chemical Dynamics*, edited by M. S. Child and M. A. Robb, Faraday Discussions Vol. 127 (Royal Society of Chemistry, Cambridge, 2004).
- ⁴*Multidimensional Quantum Dynamics: MCTDH Theory and Applications*, edited by H.-D. Meyer, F. Gatti, and G. A. Worth (Wiley-VCH, Weinheim, 2009).
- ⁵M. Eroms, M. Jungen, and H.-D. Meyer, *J. Phys. Chem. A* **114**, 9893 (2010).
- ⁶R. E. Wyatt, C. L. Lopreore, and G. Parlant, *J. Chem. Phys.* **114**, 5113 (2001).
- ⁷C. L. Lopreore and R. E. Wyatt, *J. Chem. Phys.* **116**, 1228 (2002).
- ⁸B. F. E. Curchod, I. Tavernelli, and U. Rothlisberger, *Phys. Chem. Chem. Phys.* **13**, 3231 (2011).
- ⁹T. J. Martínez, M. Ben-Nun, and R. D. Levine, *J. Phys. Chem.* **100**, 7884 (1996).
- ¹⁰S. Yang, J. D. Coe, B. Kaduk, and T. J. Martínez, *J. Chem. Phys.* **130**, 134113 (2009).
- ¹¹J. C. Burant and V. S. Batista, *J. Chem. Phys.* **116**, 2748 (2002).
- ¹²A. Kondorskiy and H. Nakamura, *J. Chem. Phys.* **120**, 8937 (2004).
- ¹³Y. Wu and M. F. Herman, *J. Chem. Phys.* **123**, 144106 (2005).
- ¹⁴W. H. Miller, *J. Phys. Chem. A* **113**, 1405 (2009).
- ¹⁵E. J. Heller, B. Segev, and A. V. Sergeev, *J. Phys. Chem. B* **106**, 8471 (2002).
- ¹⁶A. Donoso and C. C. Martens, *J. Phys. Chem. A* **102**, 4291 (1998).
- ¹⁷R. Kapral and G. Ciccotti, *J. Chem. Phys.* **110**, 8919 (1999).
- ¹⁸I. Horenko, C. Salzmann, B. Schmidt, and C. Schütte, *J. Chem. Phys.* **117**, 11075 (2002).
- ¹⁹K. Ando and M. Santer, *J. Chem. Phys.* **118**, 10399 (2003).
- ²⁰I. Horenko, M. Weiser, B. Schmidt, and C. Schütte, *J. Chem. Phys.* **120**, 8913 (2004).
- ²¹D. A. Micha and B. Thorndyke, in *A Tribute Volume in Honor of Professor Osvaldo Goscinski*, edited by J. R. Sabin and E. Brandas, *Advances in Quantum Chemistry* Vol. 47 (Academic, New York, 2004), pp. 293–314.
- ²²D. Mac Kernan, G. Ciccotti, and R. Kapral, *J. Phys. Chem. B* **112**, 424 (2008).
- ²³S. Bonella, G. Ciccotti, and R. Kapral, *Chem. Phys. Lett.* **484**, 399 (2010).
- ²⁴D. Bousquet, K. H. Hughes, D. A. Micha, and I. Burghardt, *J. Chem. Phys.* **134**, 064116 (2011).
- ²⁵J. C. Tully, *J. Chem. Phys.* **93**, 1061 (1990).
- ²⁶S. Nielsen, R. Kapral, and G. Ciccotti, *J. Stat. Phys.* **101**, 225 (2000).
- ²⁷N. Shenvi, *J. Chem. Phys.* **130**, 124117 (2009).
- ²⁸E. R. Dunkel, S. Bonella, and D. F. Coker, *J. Chem. Phys.* **129**, 114106 (2008).
- ²⁹T. Zimmermann and J. Vaníček, *J. Chem. Phys.* **132**, 241101 (2010).
- ³⁰H. Tao, B. G. Levine, and T. J. Martínez, *J. Phys. Chem. A* **113**, 13656 (2009).
- ³¹H. Frauenfelder and P. G. Wolynes, *Science* **229**, 337 (1985).
- ³²L. D. Landau, *Phys. Z. Sowjetunion* **1**, 88 (1932).
- ³³L. D. Landau, *Phys. Z. Sowjetunion* **2**, 46 (1932).
- ³⁴C. Zener, *Proc. R. Soc. London Ser. A* **137**, 696 (1932).
- ³⁵E. C. G. Stückelberg, *Helv. Phys. Acta* **5**, 369 (1932).
- ³⁶E. E. Nikitin, *Annu. Rev. Phys. Chem.* **50**, 1 (1999).
- ³⁷A. Peres, *Phys. Rev. A* **30**, 1610 (1984).
- ³⁸J. Vaníček and E. J. Heller, *Phys. Rev. E* **68**, 056208 (2003).
- ³⁹J. Vaníček, *Phys. Rev. E* **70**, 055201 (2004).

- ⁴⁰J. Vaníček, *Phys. Rev. E* **73**, 046204 (2006).
- ⁴¹W. H. Miller and F. T. Smith, *Phys. Rev. A* **17**, 939 (1978).
- ⁴²L. M. Hubbard and W. H. Miller, *J. Chem. Phys.* **78**, 1801 (1983).
- ⁴³S. Mukamel, *J. Chem. Phys.* **77**, 173 (1982).
- ⁴⁴J. M. Rost, *J. Phys. B* **28**, L601 (1995).
- ⁴⁵Z. Li, J.-Y. Fang, and C. C. Martens, *J. Chem. Phys.* **104**, 6919 (1996).
- ⁴⁶S. A. Egorov, E. Rabani, and B. J. Berne, *J. Chem. Phys.* **108**, 1407 (1998).
- ⁴⁷Q. Shi and E. Geva, *J. Chem. Phys.* **122**, 064506 (2005).
- ⁴⁸M. Wehrle, M. Šulc, and J. Vaníček, *Chimia* **65**, 334 (2011).
- ⁴⁹M. Šulc and J. Vaníček, "Accelerating the calculation of time-resolved electronic spectra with the cellular dephasing representation," *Mol. Phys.* (in press).
- ⁵⁰T. Gorin, T. Prosen, T. H. Seligman, and M. Znidaric, *Phys. Rep.* **435**, 33 (2006).
- ⁵¹D. A. Wisniacki, N. Ares, and E. G. Vergini, *Phys. Rev. Lett.* **104**, 254101 (2010).
- ⁵²I. García-Mata, R. O. Vallejos, and D. A. Wisniacki, *New J. Phys.* **13**, 103040 (2011).
- ⁵³C. Mollica and J. Vaníček, *Phys. Rev. Lett.* **107**, 214101 (2011).
- ⁵⁴M. Ceotto, S. Atahan, G. F. Tantardini, and A. Aspuru-Guzik, *J. Chem. Phys.* **130**, 234113 (2009).
- ⁵⁵G. Veble and T. Prosen, *Phys. Rev. Lett.* **92**, 034101 (2004).
- ⁵⁶E. Wigner, *Phys. Rev.* **40**, 749 (1932).
- ⁵⁷E. Zambrano and A. M. Ozorio de Almeida, *Phys. Rev. E* **84**, 045201 (2011).
- ⁵⁸I. V. Aleksandrov, *Z. Naturforsch., A: Phys. Sci.* **36**, 902 (1981).
- ⁵⁹W. Boucher and J. Traschen, *Phys. Rev. D* **37**, 3522 (1988).
- ⁶⁰C. C. Martens and J. Y. Fang, *J. Chem. Phys.* **106**, 4918 (1997).
- ⁶¹O. V. Prezhdo and V. V. Kisil, *Phys. Rev. A* **56**, 162 (1997).
- ⁶²J. Caro and L. L. Salcedo, *Phys. Rev. A* **60**, 842 (1999).
- ⁶³Q. Shi and E. Geva, *J. Chem. Phys.* **121**, 3393 (2004).
- ⁶⁴R. Grunwald, A. Kelly, and R. Kapral, in *Energy Transfer Dynamics in Biomaterial Systems*, edited by I. Burghardt, V. May, D. A. Micha, E. R. Bittner, F. Schäfer, J. Toennies, and W. Zinth, Springer Series in Chemical Physics Vol. 93 (Springer, Berlin, 2009), pp. 383–413.
- ⁶⁵N. Ananth, C. Venkataraman, and W. H. Miller, *J. Chem. Phys.* **127**, 084114 (2007).
- ⁶⁶H.-D. Meyer and W. H. Miller, *J. Chem. Phys.* **70**, 3214 (1979).
- ⁶⁷G. Stock and M. Thoss, *Phys. Rev. Lett.* **78**, 578 (1997).
- ⁶⁸V. Engel and H. Metiu, *J. Chem. Phys.* **90**, 6116 (1989).
- ⁶⁹N. van Veen, M. D. Vries, J. Sokol, T. Baller, and A. de Vries, *Chem. Phys.* **56**, 81 (1981).
- ⁷⁰M. B. Faist and R. D. Levine, *J. Chem. Phys.* **64**, 2953 (1976).
- ⁷¹M. D. Feit and J. A. Fleck, Jr., *J. Chem. Phys.* **78**, 301 (1983).
- ⁷²D. Kosloff and R. Kosloff, *J. Comput. Phys.* **52**, 35 (1983).
- ⁷³L. Verlet, *Phys. Rev.* **159**, 98 (1967).
- ⁷⁴R. MacKenzie, M. Pineault, and L. Renaud-Desjardins, *Can. J. Phys.* **90**, 187 (2012).
- ⁷⁵X. Sun and W. H. Miller, *J. Chem. Phys.* **106**, 6346 (1997).
- ⁷⁶B. Li, C. Mollica, and J. Vaníček, *J. Chem. Phys.* **131**, 041101 (2009).
- ⁷⁷J.-Y. Fang and S. Hammes-Schiffer, *J. Phys. Chem. A* **103**, 9399 (1999).
- ⁷⁸C. Y. Zhu, S. Nangia, A. W. Jasper, and D. G. Truhlar, *J. Chem. Phys.* **121**, 7658 (2004).
- ⁷⁹G. Granucci and M. Persico, *J. Chem. Phys.* **126**, 134114 (2007).
- ⁸⁰G. Granucci, M. Persico, and A. Zocante, *J. Chem. Phys.* **133**, 134111 (2010).
- ⁸¹J. E. Subotnik and N. Shenvi, *J. Chem. Phys.* **134**, 024105 (2011).
- ⁸²T. Zimmermann, J. Ruppen, B. Li, and J. Vaníček, *Int. J. Quantum Chem.* **110**, 2426 (2010).